Morio Kobayashi was born in Nagano, Japan, on March 31, 1943. He received the B.S. degree from the Science University of Tokyo, Japan, in 1967, and the M.S. degree from Osaka City University, Osaka, Japan, in 1969.

In 1969 he joined Musashino Electrical Communication Laboratory, and in 1971 he joined the Ibaraki Electrical Communication Laboratory, Nippon Telegraph and Telephone Public Corporation, Ibaraki-ken, Japan. He was initially engaged in the research of electrophotography. He is presently engaged in research on optical guided-wave devices.

Mr. Kobayashi is a member of the Institute of Electronics and Communication Engineers of Japan and the Japan Society of Applied Physics.

Hiroshi Terui was born in Aomori, Japan, on February 18, 1950. He received the B.S. and M.S. degrees in physics from Tohoku University, Japan, in 1972 and 1974, respectively.

In 1974 he joined the Ibaraki Electrical Communication Laboratory, Nippon Telegraph and Telephone Public Corporation, Ibaraki-ken, Japan, where he was engaged in research on materials for magnetooptic recording. Since 1976 he has been engaged in research on optical guided-wave devices.

Mr. Terui is a member of the Institute of Electronics and Communication Engineers of Japan and the Japan Society of Applied Physics.

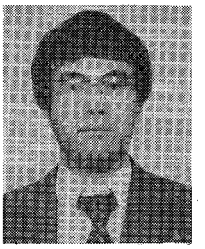

Masao Kawachi was born in Gunma, Japan, on March 17, 1949. He received the B.S. and M.S. degrees in physical electronics and the Ph.D. degree from Tokyo Institute of Technology, Tokyo, Japan, in 1971, 1973, and 1978, respectively.

In 1973 he joined the Ibaraki Electrical Communication Laboratory, Nippon Telegraph and Telephone Public Corporation, Ibaraki-ken, Japan, where he was engaged in research on liquid crystals and their application to display devices. He is presently engaged in research on optical fiber fabrication and integrated optical devices.

Dr. Kawachi is a member of the Institute of Electronics and Communication Engineers of Japan and the Japan Society of Applied Physics.

Juichi Noda, for a biography, see this issue, p. 1560.

Guided Wave Approaches to Optical Bistability

GEORGE I. STEGEMAN, MEMBER, IEEE

Abstract—**We have analyzed four different guided wave approaches to achieving a power dependent refractive index and optical bistability. These include surface plasmons at the interface between a metal and a semiconductor, symmetric surface plasmon modes guided by thin metal films, conventional single film integrated optics waveguides, and multifilm integrated optics. The relative merits of each geometry are discussed for utilizing the large cubic nonlinearities in the semiconductors GaAs and InSb. Both the mode attenuation and the minimum power required for a nonlinear phase shift of $\pi/2$ are evaluated numerically and it is shown that usable propagation distances can be obtained, even for highly lossy media such as GaAs.**

I. Introduction

THE phenomenon of optical bistability [1]-[3] has generated a great deal of interest in potential applications [4]-[6]. It occurs when a medium with an intensity dependent refractive index is placed within a resonator structure with the result that both the power reflected from and transmitted through the device are no longer linear with incident power. This can lead to two states and switching between them, regions of optical gain, etc. Devices based on this phenomenon require materials with large third order nonlinearities, interaction geometries characterized by high optical power densities and long enough propagation distances to produce useful nonlinear phase shifts, and optical resonators. With the exception of a few hybrid integrated optics devices [7]-[11] most experiments reported to date have been performed in bulk media, frequently near the focal length of a lens (to produce the necessary high power densities).

Optical waves guided by single or multiple interfaces offer an attractive approach to producing high power densities over the long propagation distances desirable for optically bistable devices based on intrinsic (material) nonlinearities. For the practical realization of such devices, there are three important factors to be considered. First, the propagation distance over which bistability is achieved should be maximized. In terms of a single device, distances $\geqslant 10^3$ optical wavelengths are desirable to facilitate coupling, etc. This is also an important consideration for stacking multiple devices into logic arrays, etc. Second, the power required for device operation should be a minimum for power dissipation and device density reasons. The minimum power is usually defined in terms of the total nonlinearly produced phase change required for a particular application; this value is usually less than $\pi/2$, which we shall adopt here as an upper limit. Third, a feedback mechanism compatible with guided wave technology is required. Distributed feedback via surface or volume gratings

Manuscript received March 4, 1982; revised May 17, 1982. This work was supported by the Office of Army Research and the Air Force Office of Scientific Research.

The author is with the Optical Sciences Center, University of Arizona, Tucson, AZ 85721.

0018-9480/82/1000-1598$00.75

has been discussed in this context by Winful *et al.* [12], [13] and appears to be one logical choice for this last requirement. In this paper we shall evaluate the minimum power for this case as well as examine the first and second factors in some detail.

Optical waves can be guided by surfaces in a number of ways. Here we shall examine and compare four. The first is surface plasmons [14] propagating along the interface between semi-infinite metallic and dielectric (or semiconductor) media. Surface plasmons can also be guided by thin metallic films [14] surrounded on both sides by dielectric media. The third case treated is light guided by single film integrated optics waveguides [15] with the nonlinear material forming the film. The final geometry consists of multilayer guiding films, one of which is the nonlinear material of interest. In this paper we examine the merits of each approach and evaluate the minimum powers required for optical bistability.

Under most practical conditions, the intensity dependent change in the propagation wave vector and, consequently, the minimum power required for bistability can be evaluated simply from coupled mode theory [16]. A number of such calculations have already been reported [17]-[19], namely for surface plasmons [17] and thin film [18] and channel waveguides [19]. Their starting point has been the planewave analog [20], [21] of a power dependent refractive index, i.e., the relation

$$n = n_0 + n_{2,E}|E|^2 \tag{1}$$

where n_0 is the unperturbed index, $n_{2,E}$ is the field dependent component, and E is the local field. In this paper we shall show that this is appropriate for pure TE guided waves, but not for modes with a TM component.

The most promising materials for reasons of high nonlinearities, integration with other integrated optics functions, compatibility with high speed electronics, etc., are semiconductors. The two most extensively studied to date are GaAs [2], [22], [23] and InSb [3], [24]-[26], neither of which has exhibited optimum nonlinearities in wavelength regions suitable for widespread applications. They do, however, provide test cases for demonstrating bistability and related effects until more suitable materials are developed. Both media exhibit loss, a feature intrinsic to highly nonlinear semiconductors. This problem is especially acute in GaAs in the wavelength region in which excitonic effects are responsible for the large measured values of n_2 [2]. In this paper we examine the effects of loss on the minimum power for bistability in these materials. Of particular interest here is the tradeoff between propagation distance and minimum power, as well as a technique for obtaining useful propagation distances in high loss materials such as GaAs.

This paper is structured as follows. In the next two sections, the form of the guided wave fields will be discussed and relations for minimum power derived. In Sections IV and V we evaluate numerically these general expressions for GaAs (IV) and InSb (V) for each of the four waveguiding geometries, and compare them. The most detailed analysis will be given for GaAs and only the optimum cases will be discussed for InSb. In the last section we briefly discuss the main results of this paper.

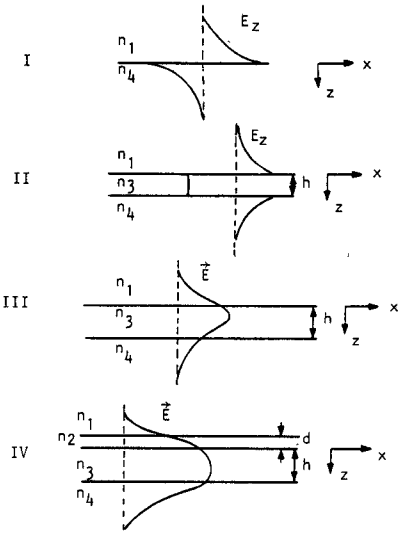

Fig. 1. The four guided wave geometries analyzed. I and II refer to surface plasmons guided by a metal-semiconductor interface and a thin metal film, respectively. III and IV refer to single and multilayer integrated optics waveguides. The nonlinear medium is n_1, n_1 and/or n_4, n_3, and n_2 in I, II, III, and IV, respectively.

II. Guided Wave Fields

The four guided wave geometries analyzed here are shown schematically in Fig. 1. For the surface plasmon cases (I and II), the fields in the nonlinear semiconductor are evanescent in character. Furthermore, we assume that the metal itself does not contribute a significant amount to the effective third order nonlinearity encountered by the surface plasmon fields. We do, however, include loss in both the metal and semiconductor by using complex dielectric constants and refractive indexes, respectively. In the integrated optics waveguides cases, we assume losses only in the semiconductors since they are the only attenuating media involved in our modeling. The pertinent material parameters are listed in Table I.

The guided wave fields are assumed to propagate along the x-axis with the z-direction normal to the waveguiding interfaces. A complex wave vector $\beta = \beta_R - i\beta_I$ is used and the effective propagation distance (i.e., distance required for the energy to decay to $1/e$ of its original value) is given by $l_{\text{eff}} = 1/2\beta_I$. For all of the cases considered here, the guided wave fields can be expressed in the general form

$$E(r, t) = \tfrac{1}{2} E e^{i\omega t} + \text{c.c.} \tag{2}$$

where

$$E_i = E_{0i} \begin{pmatrix} C_{\text{TE}} \\ C_{\text{TM}} \end{pmatrix} f_i(z)\, b(x) \tag{3}$$

$$b(x) = e^{-i\beta_R x} a(x) \tag{4}$$

and

$$a(x) = a(0)\, e^{-\beta_I x}. \tag{5}$$

Unless otherwise indicated, all of the fields correspond to a single *input* mode number and polarization. (Coupling between *input* waves of different polarization and/or different mode number gives rise to a different range of phenomena and will be considered elsewhere.) Weak generation of modes other than the input wave does, however, occur and for that case the different modes will be identified by super- and sub-

TABLE I
MATERIAL PARAMETERS USED IN THE CALCULATIONS

Material	GaAs	InSb
Wavelength	0.82μm	∿5μm
$n_{2,I}(m^2/w)$	10^{-11} [a]	(a) 10^{-7} [b] (b) 10^{-8}
n	3.6 - .0063i [c]	(a) 4.0 - .0012i [b] (b) 4.0 - .00016i
ε (copper)	-27.25 - 1.69i [d]	-1000 - 160i [e]
ε (silver)	-32 - 1.1i [d]	
d (multilayer)	200Å	1000Å
n (GaAℓAs)	3.5	
n ($Aℓ_2O_3$)	1.77	1.77
n (ZnS)		2.0
n(Nb_2O_5)	2.28	

(a) Ref. 2,25
(b) Ref. 26
(c) H.M. Gibbs, private communication
(d) Ref. 27
(e) Ref. 28

scripts (m) and (m'). The constants C_{TE} and C_{TM} are chosen so that the power carried by the mode (TE or TM, respectively) is given by $a^2(x)$ in units of watts per millimeter of wavefront, i.e., the guided wave beam is normalized to a power of 1 W in a beam width of 1 mm. $f_i(z)$ describes the field distribution in the depth dimension of the ith electric field component. For TE guided waves $\beta \cdot E_0 = 0$ and E lies along the y-axis. For TM modes (which include surface plasmons) E_0 lies in the x-z plane.

The details of the field distributions for the waveguiding geometries considered here can all be found elsewhere in the literature [14], [15]. For the general case we write (Fig. 1) the following:

medium 1 $f_i(z) = A_{i1} \exp[S_1(z+d)]$;

$$S_1^2 = \beta^2 - n_1^2 k^2 \quad (6)$$

medium 2 $f_i(z) = A_{i2}\{\cos_c[S_2(z+d)] + B_{i2} \sin_c[S_2(z+d)]\}$;

$$S_2^2 = n_2^2 k^2 - \beta^2 \quad (7)$$

medium 3 $f_i(z) = A_{i3}\{\cos_c(S_3 z) + B_{i3} \sin_c(S_3 z)\}$;

$$S_3^2 = n_3^2 k^2 - \beta^2 \quad (8)$$

medium 4 $f_i(z) = A_{i4} \exp[-S_4(z-h)]$;

$$S_4^2 = \beta^2 - n_4^2 k^2 \quad (9)$$

where n_j is the refractive index of the jth medium; the $\cos_c$ and $\sin_c$ are complex cosine and sine functions, respectively. Application of continuity of tangential electric and magnetic fields at each interface is sufficient to determine all of the field parameters A_{ij} and B_{ij}, as well as the dispersion relations. The normalization constants C_{TE} and C_{TM} are obtained from

$$\frac{1}{4}\int [ExH^* + E^*xH]_{x=0} \cdot \hat{x}\, dz = 1 \quad (10)$$

with

$$a^2(0) = 1.$$

The dispersion relations for all four cases can be obtained from two equations. For TE polarized waves

$$\tan(S_2 h) = \frac{\tan(S_3 d)\, S_2(S_4 S_1 - S_3^2) + S_2 S_3 (S_1 + S_4)}{\tan(S_3 d)\,(S_1 S_3^2 + S_2^2 S_4) + (S_2^2 - S_1 S_4) S_3} \quad (11)$$

where d and h are the two film thicknesses, respectively. For TM waves

$$\tan(S_2 h) = \frac{\tan(S_3 d)\, S_2 n_2^2 (S_1 S_4 n_3^4 - S_3^2 n_1^2 n_4^2) + S_2 S_3 n_2^2 n_3^2 (S_1 n_4^2 + S_4 n_1^2)}{\tan(S_3 d)\,(S_2^2 S_4 n_1^2 n_3^4 + S_1 S_3^2 n_2^4 n_4^2) + S_3 n_3^2 (S_2^2 n_1^2 n_4^2 - S_1 S_4 n_2^4)}. \quad (12)$$

In the case of a single film (II and III), $d = 0$. For case I, $d = h = 0$. The first step in our analysis was to solve the appropriate dispersion relation (11) or (12) for the complex β. This was done numerically.

III. INTENSITY DEPENDENT REFRACTIVE INDEX EFFECTS

When an optical field propagates in a medium characterized by a third order nonlinearity, i.e., cubic in the incident field E, a nonlinear polarization field of the form [20], [21]

$$P_i = 6C_{1122}(-\omega, \omega, \omega, -\omega) E_i E_j E_j^* + 3C_{1221}(-\omega, \omega, \omega, -\omega) E_i^* E_j E_j \quad (13)$$

is generated at the incident field frequency. Here C_{1122} and

C_{1221} are the usual [20], [21] third order nonlinear coefficients. Equation (13) can be rewritten in terms of $n_{2,E}$ as

$$P_i = 2n_0 n_{2,E} \{\tfrac{2}{3} E_i E_j E_j^* + \tfrac{1}{3} E_i^* E_j E_j\}. \tag{14}$$

The effect of this polarization on the incident optical field can easily be evaluated from coupled mode theory [16], i.e.,

$$\frac{d}{dx} a(x) + \beta_I a(x) = \frac{kc\epsilon_0}{4i} \int P_i E_{0i}^* \begin{pmatrix} C_{\mathrm{TE}} \\ C_{\mathrm{TM}} \end{pmatrix} f_i^*(z)\, dz \exp(i\beta_R x)$$

$$= -i\Delta\beta(x)\, a(x). \tag{15}$$

The parameter $\Delta\beta(x)$ is the intensity dependent change in the propagation wave vector which is in turn written as

$$\Delta\beta(x) = \Delta\beta_0 a^2(0)\, e^{-2\beta_I x} \tag{16}$$

with

$$\Delta\beta_0 = \frac{kc\epsilon_0}{2} \int \begin{pmatrix} C_{\mathrm{TE}} \\ C_{\mathrm{TM}} \end{pmatrix}^4 n_0(z)\, n_{2,E}(z) \left[\frac{2}{3} |f_i(z)|^2 |f_j(z)|^2 \right.$$

$$\left. \cdot |E_{0i} E_{0i}^*| |E_{0j} E_{0j}^*| + \frac{1}{3} f_i^*(z)^2 f_j(z)^2 E_{0i}^{*2} E_{0j}^2 \right] dz. \tag{17}$$

The solution to (15) is

$$b(x) = b(0) \exp - i(\beta + \Delta\beta(x))x \tag{18}$$

which is the rationale for the interpretation of $\Delta\beta(x)$. Note that not only is the real part of the propagation wave vector changed, but additional loss occurs due to $\Delta\beta_I(x)$—this contribution to the attenuation is usually negligible. For TE polarized modes, (17) reduces to

$$\Delta\beta_0 = \frac{kc\epsilon_0}{2} \int n_0(z)\, n_{2,E}(z)\, |f_y(z)|^4\, C_{\mathrm{TE}}^4 |E_{0y}|^4\, dz. \tag{19}$$

This is equivalent to writing $P_i = \Delta\epsilon E_i$ with $\Delta\epsilon = n^2 - n_0^2$, using (1) for n, and substituting P_i into (15). For TM modes,

$$\Delta\beta_0 = \frac{kc\epsilon_0}{2} \int n_0(z)\, n_{2,E}(z)\, C_{\mathrm{TM}}^4 \left[\frac{2}{3}(|f_x(z)|^2\, |E_{0x}|^2 \right.$$

$$\left. + |f_z(z)|^2\, |E_{0z}|^2)^2 + \frac{1}{3} |f_x^2(z) E_{0x}^2 + f_z^2(z) E_{0z}^2|^2 \right] dz \tag{20}$$

which does *not* in general reduce to

$$\Delta\beta_0 = \frac{kc\epsilon_0}{2} \int n_0(z)\, n_{2,E}(z)\, C_{\mathrm{TM}}^4 (|f_x(z)|^2\, |E_{0x}|^2$$

$$+ |f_z(z)|^2\, E_{0z}|^2)^2\, dz \tag{21}$$

unless $f_x(z) E_{0x}$ and $f_z(z) E_{0z}$ are in phase. For example, for evanescent fields $f_x(z) E_{0x}$ and $f_z(z) E_{0z}$ are $\pi/2$ out of phase and an error of 50 percent in $\Delta\beta_0$ can result if (21) instead of (20) is used and if the second term in the brackets in (20) is zero. Hence, we conclude that (21) is not strictly valid for modes with field components along the propagation, wave vector, i.e., surface plasmons [17], TM integrated optics waveguides [18], and channel waveguides [19] in general.

For optically bistable devices it is the total nonlinearly produced phase shift for a propagation distance l which is important, i.e.,

$$\Delta\phi = \int_0^l \Delta\beta(x)\, dx. \tag{22}$$

The maximum $\Delta\phi$ required is $\pi/2$, although for most applications involving resonators it is much less (depending on the "Q" of the cavity). Hence, we set $\Delta\phi = \pi/2$ as an upper limit. Furthermore, the maximum phase shift occurs for $l \to \infty$. Therefore,

$$\frac{\pi}{2} = \int_0^\infty \Delta\beta(x)\, dx \tag{23}$$

which gives

$$a_m^2(0) = \pi\beta_I / \Delta\beta_0 \tag{24}$$

for the minimum power required to produce a $\pi/2$ phase shift. To obtain this phase shift over the distance $l_{\mathrm{eff}} = 1/2\beta_I$, the minimum power must be increased by the factor $e/(1 - e) \simeq 1.6$. If N devices, each requiring a $\pi/2$ phase shift, are required, this minimum power must be multiplied by a factor of N. For the case of distributed feedback discussed by Winful *et al.* [12] it can easily be shown that

$$a_m^2(0) = \frac{4\beta_I}{3\Delta\beta_0}. \tag{25}$$

Coupled mode theory [16] also predicts that other guided modes of the same polarization are generated by this nonlinear polarization field. Defining the incident field as (m) and the generated field as (m'),

$$\frac{d}{dx} a_{m'}(x) + \beta_I^{(m')} a_{m'}(x) = \frac{kc\epsilon_0}{4i} \int P_i^{(m)} E_{0i}^{*(m')} \begin{pmatrix} C_{\mathrm{TE}}^{m'} \\ C_{\mathrm{TM}}^{m'} \end{pmatrix}$$

$$\cdot f_i^{*(m')}(z)\, dz \exp(i\beta_R^{(m')} x). \tag{26}$$

This can be expressed in the form

$$\frac{d}{dx} a_{m'}(x) + \beta_I^{(m')} a_{m'}(x) = F$$

$$\exp[i(\beta_R^{(m')} - \beta_R^{(m)})\, x - 3\beta_I^{(m)} x]\, a_m^3(0) \tag{27}$$

where

$$F = \frac{kc\epsilon_0}{2i} \int \begin{pmatrix} C_{\mathrm{TE}}^m \\ C_{\mathrm{TM}}^m \end{pmatrix}^3 \begin{pmatrix} C_{\mathrm{TE}}^{m'} \\ C_{\mathrm{TM}}^m \end{pmatrix} n_0(z)\, n_{2,E}(z) \left[\frac{2}{3} |f_j^{(m)}(z)|^2 \right.$$

$$\cdot f_i^{(m)}(z) f_i^{*(m')} |(z) E_{0j}^{(m)}|^2\, E_{0i}^{(m)} E_{0i}^{*(m')} + \frac{1}{3} f_j^{(m)2}(z)$$

$$\left. \cdot f_i^{*(m)}(z) f_i^{*(m')}(z)\, E_{0j}^{(m)2} E_{0i}^{*(m)} E_{0i}^{*(m')} \right] dz. \tag{28}$$

The solution is

$$a_{m'}(x) = \frac{F a_m^3(0)}{i(\beta_R^{(m')} - \beta_R^{(m)}) - 3\beta_I^{(m)} + \beta_I^{(m')}}$$

$$\cdot \{\exp[i(\beta_R^{(m')} - \beta_R^{(m)})\, x - 3\beta_I^{(m)} x] - \exp(-\beta_I^{(m')} x)\}. \tag{29}$$

Usually, $\beta_R^{(m')} \neq \beta_R^{(m)}$ and the amount of energy converted into mode m' is not significant.

There are definitely limits to the range of validity of this perturbation approach. The guided wave vector lies between two extremes β_{c0} and β_M, where β_{c0} is the mode cutoff and β_M is the maximum value. For example, for a thin film waveguide $\beta_{c0} = n_s k$ and $\beta_M = n_f k$, where n_s and n_f are the substrate and film refractive indexes, respectively. The results derived here are valid where $\beta - \beta_{c0} \gg \Delta\beta_0$ and $\beta_M - \beta \gg \Delta\beta_0$, i.e., when the field distribution associated with a mode with wave vector β is valid for the perturbed as well as unperturbed field.

IV. Guided Waves in GaAs

In this section we shall examine the minimum power and maximum propagation distance for the four guided wave configurations I-IV (Fig. 1) using GaAs as the test material. The pertinent material constants are listed in Table I. Note that we assume a complex refractive index for GaAs appropriate to 77 K with a typical planewave propagation distance of 10 μm (a factor of 10 larger than at room temperature).

A. Semi-Infinite Surface Plasmons

These waves are guided by the interface between a metal (negative dielectric constant) and the semiconductor (positive dielectric constant). As indicated in Fig. 1 [and by (6) and (9)], the fields decay exponentially into both the metal and the semiconductor and, hence, both media contribute to the propagation loss. The dispersion relation is quite simple in this case, i.e., ($\epsilon = n_4^2$ = metal dielectric constant)

$$\beta = \beta_R - i\beta_I = k\left[\frac{n_1^2\epsilon}{\epsilon + n_1^2}\right]^{1/2} \tag{30}$$

and

$$S_1 = \frac{n_1^2 k}{[-\epsilon - n_1^2]^{1/2}}, \qquad S_4 = k\left[\frac{-\epsilon}{1 + n^2/\epsilon}\right]^{1/2}. \tag{31}$$

For copper or silver metal with GaAs at $\lambda = 0.82$ μm, S_1^{-1} and S_4^{-1} both correspond to penetration distances of $\sim 0.02 \rightarrow 0.04$ μm, i.e., very strong confinement. Since the losses in the metal dominate, the propagation distances $(1/2\beta_I)$ are very small, 0.42 and 0.96 μm for copper and silver, respectively. Such short distances preclude the use of these modes at $\lambda = 0.82$ μm, and in the visible in general.

It is nevertheless instructive to evaluate the minimum power for this case to compare with previous calculations [17]. Since nonlinear effects in metals are in general very weak, we assume only the semiconductor contributes to the nonlinear phase shift (17). Evaluating (24) (for the only geometry which gives simple analytical results)

$$a_m^2(0) = \frac{8\pi\beta_I S_{1R} k^3 c^3 \epsilon_0^3 |n_1|^7}{n_{2,E} C_{TM}^4 \left[|S_1|^4 + |\beta^4| + \frac{4}{3}|S_1|^2|\beta|^2 + \frac{1}{3}S_1^2\beta^{*2} + \frac{1}{3}S_1^{*2}\beta^2\right]} \tag{32}$$

with

$$C_{TM}^2 = \frac{4kc\epsilon_0}{\frac{1}{2S_{1R}}\left[(\beta/n_1^2) + (\beta^*/n_1^{*2})\right] + \frac{1}{2S_{4R}}\left[(\beta/n_4^2) + (\beta^*/n_4^{*2})\right]} \tag{33}$$

and

$$S_1 = S_{1R} + iS_{1I}, S_4 = S_{4R} + iS_{4I}.$$

For copper and silver, the values of $a_m^2(0)$ are 382 and 274 mW/mm, respectively. This calculated value for copper is larger by a factor of 600 than that reported previously [17] (using equivalent definitions for $\Delta\phi$). Furthermore, since the fields are evanescent this is a useful case for comparing the error introduced by using (21) instead of (20). For silver, (21) leads to 199 versus 274 mW/mm from (20).

In addition to the minimum power and the maximum propagation distance, it is useful to compare $\Delta\beta_0$ for each guiding geometry. This quantity is a good indicator of the efficiency of the nonlinear interaction, independent of the distance over which the interaction can be used. From (24), $\Delta\beta_0$ has the units of watts^{-1}. For silver and copper interfaces, $\Delta\beta_0 = 5.97 \times 10^3$ W^{-1} and 9.79×10^3 W^{-1}, respectively.

B. Surface Plasmons Guided by Metal Films

Surface plasmon-like modes can also be guided by thin metal films ($n_1 \geqslant n_4$). The pertinent dispersion relations and field distributions are described by TM polarized integrated optics with the metal films playing the role of the guiding film. The number (maximum of two) and types of modes which can exist are determined by the relative values of the refractive indexes ($d = 0$ in Fig. 1). The important factors are the wave vectors β_1 and β_4 for the surface plasmons which would exist at the n_1-n_3 and n_4-n_3 interfaces when the metal film thickness becomes infinite, i.e., much larger than the skin depth associated with each interface. An "antisymmetric" mode with $\beta > \beta_1$ always exists and is characterized by attenuation larger than that for surface plasmons propagating along the interface between the semi-infinite media n_1 and n_3. As the film thickness increases, this mode becomes progressively more localized at the n_1-n_3 interface. A "symmetric" mode exists in the region $n_1 k > \beta > \beta_4$ as long as $n_1 k > \beta_4$, otherwise it does not exist. As the metal thickness increases this mode becomes progressively more localized at the n_3-n_4 boundary, i.e., $\beta \rightarrow \beta_4$ as $h \rightarrow \infty$. As the film thickness decreases, the fields penetrate progressively deeper into the medium n_4 and the losses due to the metal decrease. At cutoff for this mode, the loss is governed totally by the medium n_4. For GaAs, $1/2\beta_I$ approaches 10 μm asymptotically. Hence, for this symmetric mode, the attenuation varies between the semi-infinite surface plasmon and the planewave in medium n_4 values. It is this low-loss mode which we examine further.

The metals which exhibit the lowest losses are also those which are the most difficult to fabricate as continuous smooth metal films. Silver, for example, forms islands during deposition which do not coalesce into continuous films until "average" film thicknesses of $\sim$150 Å are reached. Since continuous films are necessary for surface plasmon propagation, we assume that minimum thicknesses of 150 Å are required.

(Surface roughness could be an additional complication which reduces the propagation distance.)

We first evaluate the propagation distance for a number of cases [Fig. 2(b)]. For the symmetric case ($n_1 = n_4$), a maximum propagation distance of ~6 μm is feasible at $h \simeq 150$ Å. (If there was no loss in the GaAs this would increase to ~20 μm.) When $n_1 \neq n_4$, the propagation distance increases to ~9 μm at $h = 150$ Å if the non-GaAs material is assumed to be lossless (for $|n_1 - n_4| = 0.1$). Hence, for all of these cases, the usable propagation distances are of the order of 10 optical wavelengths, i.e., ~8 μm and the attenuation approaches asymptotically the semi-infinite surface plasmon value for thick films. These distances do not appear to be adequate for practical applications.

The variation in the minimum power with film thickness is shown in Fig. 2(a) (with $n_1 \geqslant n_4$ assumed throughout). As expected, the optimum (210 mW/mm) occurs for the hypothetical case of no loss in GaAs. For the symmetric case, including loss, the minimum power is 690 mW/mm at $h =$ 150 Å and it approaches asymptotically the value 540 mW/mm for thick films. For $n_{GaAs} > n_4$, the mode tends to be localized at the interface of the medium opposite to the GaAs and hence, the minimum powers are high and grow rapidly with increasing thickness. For $n_1 > n_{GaAs}$, the energy localizes with increasing film thickness at the n_3-n_4 interface and the minimum power decreases asymptotically to the semi-infinite medium surface plasmon value.

The parameter $\Delta\beta_0$ varies with film thickness. Its optimum value coincides with that of the semi-infinite surface plasmon case for which the field confinement is an optimum.

C. Single Film Integrated Optics

As is well known [15], waves can be guided by multireflection effects in a thin film surrounded on both sides with media of a lower refractive index. Here we consider a GaAs film grown onto either a sapphire ($n_4 = 1.77$) or a GaAlAs ($n_4 = 3.5$) substrate. There exists a cutoff thickness below which the mode will not exist; this thickness depends on the relative value of the refractive indexes, the mode polarization, and the mode number. For a given mode, the fraction of energy carried by the film increases from 0-100 percent as the film thickness is increased from cutoff. This is indicated in Fig. 3(b) for both mode polarizations and different mode numbers.

The minimum power was calculated using the formalism outlined in Section III and the results are shown in Fig. 3(a). This geometry for the TE_0 mode yields the lowest minimum powers for the four configurations analyzed (~150 mW/mm). At $h \sim 350$ Å, a propagation distance of 22 μm is feasible. Although this value is still not of practical magnitude, this geometry is more promising than the ones utilizing surface plasmons.

The variation in minimum power with mode polarization and number is also shown in Fig. 3(a). Since thicker films are required to support TM polarized modes and higher order TE modes, the incident wave power is not utilized as efficiently as for the TE_0 case with the result that the minimum powers required are larger than for the TE_0 case. Furthermore, when the refractive index between the film (GaAs) and the substrate is decreased (e.g. for GaAlAs), the cutoff thickness (and hence the minimum power) increases. This is unfortunate because GaAs can be grown successfully on GaAlAs, but the minimum power for this case is ~ 800 mW/mm.

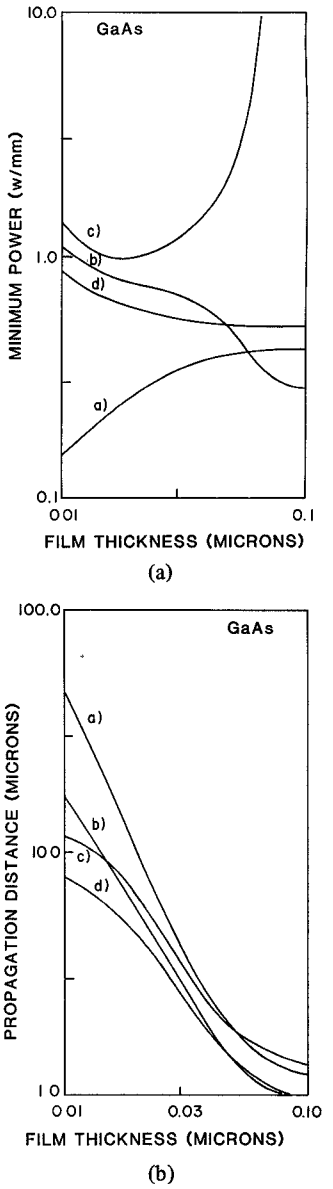

Fig. 2. (a) The minimum power for a $\pi/2$ phase shift and (b) the maximum propagation distance for surface plasmons guided by a thin silver film of variable thickness. The curves *a*, *b*, *c*, and *d* refer to geometry II (Fig. 1) with *a*, no loss in the GaAs and $n_1 = n_4 = n_{GaAs}$; *b*, $n_1 = 3.7$ and $n_4 = n_{GaAs}$; *c*, $n_1 = n_{GaAs}$ and $n_4 = 3.5$; *d*, $n_1 = n_4 = n_{GaAs}$.

The parameter $\Delta\beta_0$ varies with film thickness, mode number, and mode polarization. The largest value of 0.82×10^3 W^{-1} occurs for a TE_0 mode at a GaAs film thickness of ~700 Å. This value is approximately one order of magnitude smaller than for the optimum surface plasmon cases.

D. Multifilm Integrated Optics

Light can be guided by multifilm structures (Fig. 1), as long as the refractive indexes of media n_1 and n_4 are less than that of the film (n_2 or n_3) responsible for the guiding. By using

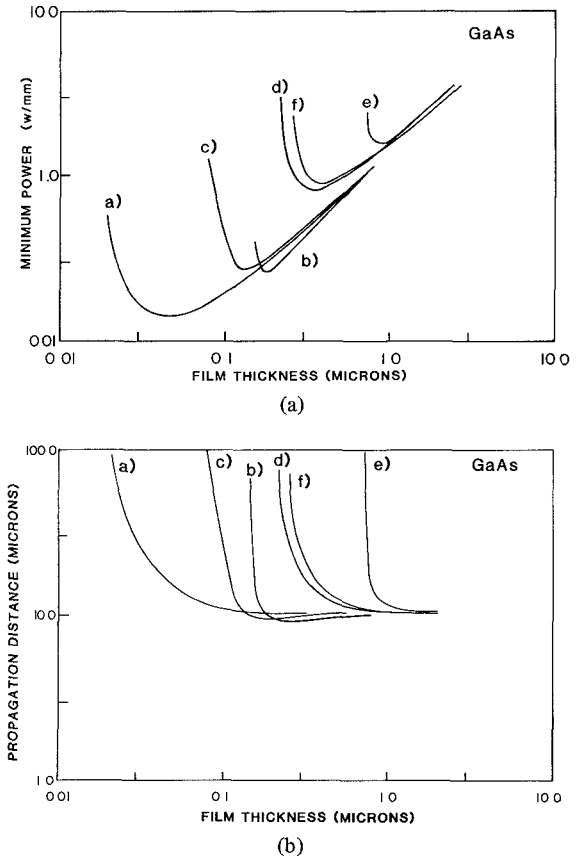

Fig. 3. (a) The minimum power for a $\pi/2$ phase shift and (b) the maximum propagation distance for waves guided by a thin film of variable thickness of GaAs deposited on an Al_2O_3 substrate *a–c* and an GaAlAs substrate *d–f*. *a*–TE_0; *b*–TE_1; *c*–TM_0; *d*–TE_0; *e*–TE_1; and *f*–TM_0.

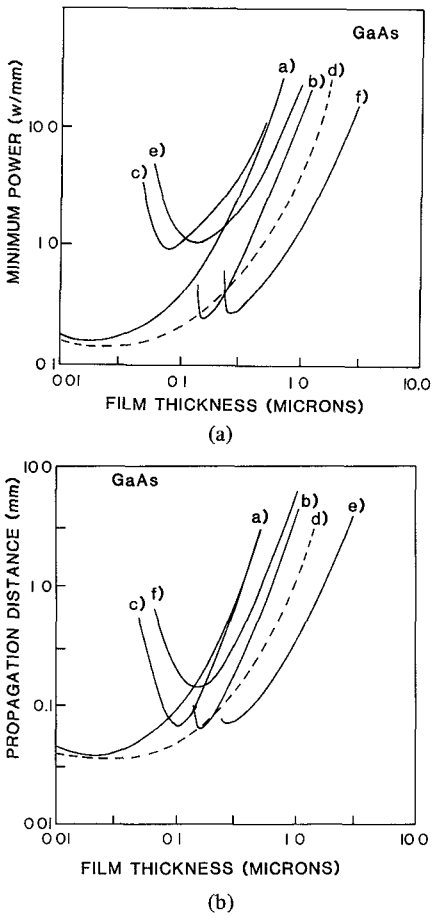

Fig. 4. (a) The minimum power for a $\pi/2$ phase shift and (b) the maximum propagation distance for waves guided by a 200 Å film of GaAs deposited on an GaAlAs – Al_2O_3 (*a*, *b*, *c*) and an Nb_2O_5 – SiO_2 (*d*, *e*, *f*) waveguide. *a*–TE_0; *b*–TE_1; *c*–TM_0; *d*–TE_0; *e*–TE_1; and *f*–TM_0.

such a two film waveguide, it is possible to vary both the propagation distance and minimum power. We do not carry out such an exercise here, but rather examine two cases and discuss the resulting tradeoffs.

The variation in propagation distance with film thickness is shown in Fig. 4(b). We assumed a constant GaAs thickness of 200 Å and variable thickness for guiding films of niobium oxide ($n_3 = 2.28$) and GaAlAs ($n_3 = 3.5$). For TE_0 modes, the minimum propagation distances are of the order of 35 μm. For TM polarization, and for increasing mode number, the minimum propagation distances are larger because the cutoff thickness for these cases require thicker films and hence, a smaller fraction of the mode energy is carried by (and dissipated in) the GaAs film. However, the most salient result of Fig. 4(b) is that the propagation distance can be increased to millimeter + values, compatible with a guided wave approach. These values are useful for device purposes.

This increase in propagation distance comes at the expense of an increase in minimum power. The numerical results are shown in Fig. 4(a). Near the minimum in the propagation distance, the corresponding minimum powers are ~140 mW/mm, comparable to the single thin film case. Of more interest is the minimum power for a propagation distance of, for example, 1 mm. For both cases, TE_0 mode values are ~3-4 W/mm. For TM modes, as well as higher order numbers, this minimum power increases. Inspection of the curves in Fig. 4(a) and (b) shows that the minimum power increases linearly with propagation distance, as long as the curves are far from their minima.

As noted in the previous cases $\Delta\beta_0$ depends on the film thicknesses assumed. For the two cases considered here, $\Delta\beta_0 \simeq 0.32 \times 10^3 W^{-1}$. This value is lower than for the single film case, primarily because part of the guided wave power is carried by the second film and hence is not useful for the nonlinear interaction.

V. Guided Waves in Indium Antimonide

The semiconductor indium antimonide in the vicinity of its bandgap (~5 μm) exhibits some of the largest cubic nonlinearities of any material reported to date [24]-[26]. Similar to the previously discussed GaAs case, liquid nitrogen temperatures are required to minimize the attenuation in InSb. The variation with wavelength of both the planewave attenuation and the cubic nonlinearity have been measured in this material [26] and we shall examine here the cases for the two wavelengths at which $n_{2,I} = 10^{-6}$ m^2/W and 10^{-7} m^2/W. (The pertinent material constants are listed in Table I.)

The numerical results for both the propagation distance and the minimum power are summarized in Fig. 5. (The details of different cases are similar to those discussed in the last

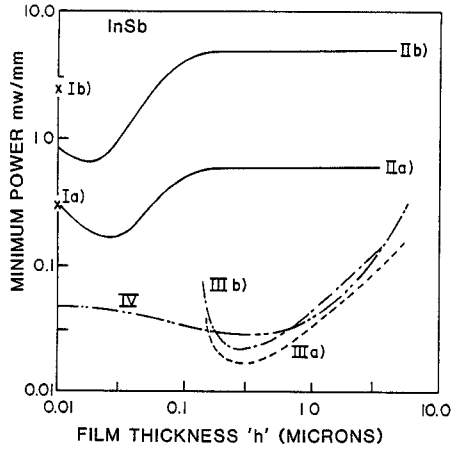

(a)

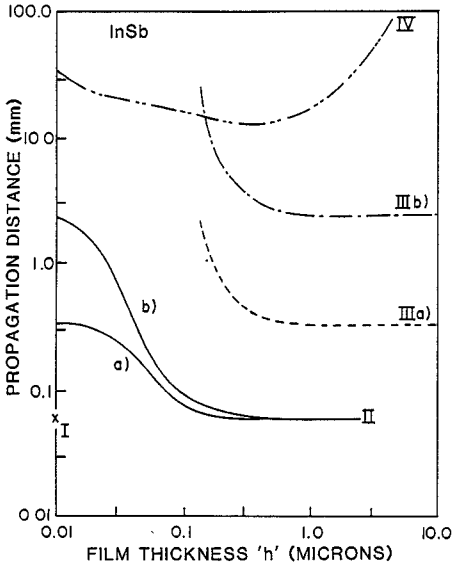

(b)

Fig. 5. (a) The minimum power for a $\pi/2$ phase shift and (b) the maximum propagation distance for *I* surface plasmons guided by an InSb-copper interface (indicated by *X*); II surface plasmons guided by a copper film surrounded by InSb; III waves guided by a thin film of InSb deposited on ZnS; and IV waves guided by a 1000 Å layer of InSb on a ZnS-Al_2O_3 waveguide. The parameters pertinent to (a) and (b) are defined in Table I.

section for GaAs, and will not be repeated here.) For surface plasmons at the interface between InSb and copper, most of the mode energy is carried outside the metal even though the dissipation in the metal still constitutes the major loss mechanism. The propagation distances at the two wavelengths are 65-82 μm, which correspond to 13-16λ. The minimum power, however, is approximately inversely proportional to the magnitude of $n_{2,E}$ and takes the values 0.29 and 2.4 mW/mm, respectively, for $n_{2,I} = 10^{-6}$ m^2/W and $n_{2,I} = 10^{-7}$ m^2/W. These results are in excess of five orders of magnitude larger than previously reported [17].

The results for symmetric surface plasmons guided by thin copper films in a symmetric medium geometry are shown in Fig. 5. For feasible film thicknesses ($h \geq 150$ Å), there is a tradeoff between propagation distance and minimum power. For the higher $n_{2,E}$, a minimum power of 170 μW/mm can be obtained with a propagation distance of ~0.3 mm. For the lower nonlinearity, a distance of 1.5 mm (300λ) should be possible, with a corresponding increase to a minimum power of 650 μW/mm. Both of these cases could be useful for device applications if the waves could be launched by focusing 5 μm radiation onto a transverse face of the waveguide.

The predictions for a single film integrated optics waveguide (TE_0 mode) appear quite promising. A minimum power as low as 11 μW/mm should be feasible with propagation distances of 0.5 mm. Operating with the reduced nonlinearity (and loss), a propagation distance of 6.5 mm (~1300λ) is predicted with a moderate increase in minimum power to 25 μW/mm. Such distances (>1000λ) are promising for efficient grating or prism coupling.

Utilization of multifilm waveguides can increase the propagation distance into the multicentimeter range. For example, using an air-InSb (1000 Å)-ZnS-Al_2O_2 (substrate) composite structure, a 5 cm distance can be achieved with a minimum power of only 0.1 mW/mm. Such a long distance ($10^4\lambda$) is well-suited for easy coupling via prisms or gratings, and this combination looks very attractive for experimental work.

We also evaluated the parameter $\Delta\beta_0$. The maximum value for the surface plasmon cases is 0.87×10^5 W^{-1}. This increases to 1.96×10^5 W^{-1} for a single indium antimonide film waveguide and decreases to 0.20×10^5 W^{-1} for the multilayer case.

The surface plasmon case provides an example in which the perturbation analysis presented here is not strictly valid. Here $\beta - \beta_{c0}/\beta < 0.008$ for all cases. Since $\Delta\beta_0/\beta = \lambda/4l_{\text{eff}}$, $\Delta\beta_0/\beta \sim 0.015$ for the semi-infinite medium case. Furthermore, the criterion $\Delta\beta_0 < \beta - \beta_{c0}$ is only marginally satisfied for surface plasmons guided by thin metal films.

VI. Discussion

We are now in a position to compare the four guided wave approaches to producing nonlinearly produced phase shifts. In general, surface plasmons guided at the interface between a metal and a semiconductor do not provide an attractive mode for achieving optical bistability. Although the minimum powers are marginally larger (but of the same order of magnitude) than those predicted for the other three approaches, the propagation distances are just too small to be practical. Guiding the radiation by thin metal films leads to much longer propagation distances and comparable minimum powers. The attenuation in this second case lies between that for planewaves in the semiconductor, and that for surface plasmons at the interface between semi-infinite media. It is ultimately this attenuation which will limit the applicability of these metal film guided surface plasmons.

Thin film integrated optics appears to provide the optimum approach to efficiently produced nonlinear phase shifts coupled with reasonably large propagation distances. Optimum minimum powers are obtained by making the guiding film a thin film waveguide out of the nonlinear material. Propagation distances 2-3 times the planewave value occur at these optimum points. These propagation distances can be made even larger by using two-layer guiding films. Even for GaAs which is very lossy, propagation distances in excess of millimeters are predicted. The increase in distance is a conse-

quence of the fraction of mode energy carried by the lossy semiconductors being decreased relative to the single film case. This also results in an increase in the minimum power because less of the mode is affected by the nonlinearity. Such multilayer waveguides allow the propagation distances to be made in excess of $10^3\lambda$, a distance we consider useful for launching modes using standard integrated optics coupling techniques.

The high degree of confinement provided by guided wave structures cannot be achieved anywhere else but in the focal regions of a lens. In that case, the confinement cannot be maintained over long propagation distances. Hence, guided waves should ultimately lead to the most efficient devices.

In terms of demonstrating very efficient optical bistability in a guided wave context, InSb appears to be the best candidate. The present calculations have also been extended to channel waveguides with widths typically 1 μm or less. In these cases, the minimum powers are reduced by a further factor of $>10^3$. For InSb, this led to minimum calculated powers of <10 nW, and for GaAs to ~ 50 μW.

In this work we have concentrated on three specific wavelengths and have not addressed in detail the tradeoffs between the nonlinearity n_2, the loss α, the propagation distance, and the power required for bistability. In the case of GaAs, n_2 is known only near the exciton feature [2], [25] (the case examined here), and at 1.06 μm where the value [29] of n_2 is relatively small, i.e., $10^{-18} \rightarrow 10^{-19}$ W/m^2 and high power lasers are required to observe bistable behavior. The situation is better for InSb where Smith [26] and co-workers have measured both n_2 and α in the vicinity of the bandgap. In the present calculation, n_2 and α at $\sim 1840^{-1}$ and ~ 1760 cm^{-1} were used. The results in Fig. 5(a) indicate that $n_2/\alpha \simeq$ constant and hence, the power required for a $\pi/2$ phase shift is comparable for the two cases, despite the large difference in propagation distance [Fig. 5(b)].

Acknowledgment

The author gratefully acknowledges contributions from H. Gibbs and D. Smith.

References

[1] An excellent review is provided by *Optical Bistability*, C. Bowden, M. Ciftan, and H. Robl, Eds. New York: Plenum, 1981; also *IEEE J. Quantum Electron.*, vol. QE-17, Mar. 1981.

[2] H. M. Gibbs, S. L. McCall, T.N.C. Venkatesan, A. C. Gossard, and W. Wiegmann, "Optical bistability in semiconductors," *Appl. Phys. Lett.*, vol. 35, pp. 451–453, 1979.

[3] D.A.B. Miller, S. D. Smith, and A. Johnston, "Optical bistability and signal amplification in a semiconductor crystal: Applications of new low-power nonlinear effects in InSb," *Appl. Phys. Lett.*, vol. 35, pp. 658–660, 1979.

[4] P. W. Smith, "Hybrid bistable optical devices," *Opt. Eng.*, vol. 19, pp. 456–462, 1980.

[5] H. M. Gibbs, S. L. McCall, and T.N.C. Venkatesan, "Optical bistable devices: The basic components of all-optical systems?," *Opt. Eng.*, vol. 19, pp. 463–468, 1980.

[6] P. W. Smith and W. J. Tomlinson, "Bistable optical devices promise subpicosecond switching," *IEEE Spectrum*, vol. 18, no. 6, pp. 26–33, 1981.

[7] P. W. Smith, I. P. Kaminow, P. J. Maloney, and L. W. Stulz, "Integrated bistable optical devices," *Appl. Phys. Lett.*, vol. 33, pp. 24–26, 1978; and "Self-contained integrated bistable optical devices," *Appl. Phys. Lett.*, vol. 34, pp. 62–65, 1979.

[8] E. Garmire, S. D. Allen, J. Marburger, and C. M. Verber, "Multimode integrated optical bistable switch," *Opt. Lett.*, vol. 3, pp. 69–71, 1978.

[9] P. S. Cross, R. V. Schmidt, R. L. Thornton, and P. W. Smith, "Optically controlled two channel integrated-optical switch," *IEEE J. Quantum Electron.*, vol. QE-14, pp. 577–580, 1978.

[10] A. Schapper, M. Papuchon, and C. Puech, "Optical bistability using an integrated two arm interferometer," *Opt. Commun.*, vol. 29, pp. 364–368, 1979.

[11] H. Ito, Y. Ogawa, and H. Inaba, "Analyses and experiments on integrated optical multivibrators using electrooptically controlled bistable optical devices," *IEEE J. Quantum Electron.*, vol. QE-17, pp. 325–331, Mar. 1981.

[12] H. G. Winful, J. H. Marburger, and E. Garmire, "Theory of bistability in nonlinear distributed feedback structures," *Appl. Phys. Lett.*, vol. 35, pp. 379–381, 1979.

[13] H. G. Winful, "Optical bistability in periodic structures and in degenerate four-wave mixing," in *Proc. Int. Conf. on Excited States and Multiresonant Nonlinear Optical Processes in Solids*, Aussois, France, 1981, pp. 55–58.

[14] E. N. Economou, "Surface plasmons in thin films," *Phys. Rev.*, vol. 182, pp. 539–554, 1969.

[15] P. K. Tien, "Integrated optics and new wave phenomena in optical waveguides," *Rev. Mod. Phys.*, vol. 49, pp. 361–420, 1977.

[16] D. Marcuse, *Theory of Dielectric Optical Waveguides*, New York: Academic, 1974; also H. Kogelnik, *Integrated Optics, Vol. 7 of Topics in Applied Physics*, T. Tamir, Ed., Berlin: Springer-Verlag, 1975, pp. 66–79.

[17] D. Sarid, "The nonlinear propagation constant of a surface plasmon," *Appl. Phys. Lett.*, vol. 39, pp. 889–891, 1981.

[18] D. Sarid and G. I. Stegeman, "Optimization of the effects of power dependent refractive indices in optical waveguides," *J. Appl. Phys.*, vol. 52, pp. 5439–5441, 1981.

[19] D. Sarid, "Analysis of bistability in a ring-channel waveguide," *Opt. Lett.*, vol. 6, pp. 552–554, 1981.

[20] P. D. Maker and R. W. Terhune, "Study of optical effects due to an induced polarization third order in the electric field strength," *Phys. Rev.*, vol. 137, pp. A801-818A, 1965.

[21] R. W. Hellwarth, "Third order optical susceptibilities of liquids and solids," in *Progress in Quantum Electronics*, J. H. Sanders and S. Stenholm, Eds. New York: Pergamon, 1977, vol. 5, pp. 1–68.

[22] H. M. Gibbs, A. C. Gossard, S. L. McCall, A. Passner, W. Wiegmann, and T.N.C. Venkatesan, "Saturation of the free exciton resonance in GaAs," *Solid State Commun.*, vol. 30, pp. 271–275, 1979.

[23] J. L. Jewell, H. M. Gibbs, S. S. Tarng, A. C. Gossard, and W. Wiegmann, "Regenerative pulsations from an intrinsic bistable optical device," *Appl. Phys. Lett.*, vol. 40, pp. 291–293, 1982.

[24] D.A.B. Miller, S. D. Smith, and A. Johnston, "Two beam optical signal amplification and bistability in InSb," *Opt. Commun.*, vol. 31, pp. 101–104, 1979.

[25] D.A.B. Miller, S. D. Smith, and C. T. Seaton, "Optical bistability in semiconductors," *IEEE J. Quantum Electron.*, vol. QE-17, pp. 312–317, Mar. 1981.

[26] D.A.B. Miller, C. T. Seaton, M. E. Prise, and S. D. Smith, "Band-gap resonant nonlinear refraction in III-V semiconductors," *Phys. Rev. Lett.*, vol. 47, pp. 197–200, 1981.

[27] P. B. Johnson and R. W. Christy, "Optical constants of the noble metals," *Phys. Rev. B.*, pp. 4370–4379, 1972; also T. Hollstein, U. Kreibig, and F. Leis, "Optical properties of Cu and Ag in the intermediate region between pure drude and interband absorption," *Phys. Status Solidi*, vol. 82, pp. 545–556, 1977; also G. Hass and L. Hadley, "Optical properties of metals," in *The A.I.P. Handbook*, D. E. Gray, Ed. New York: McGraw-Hill, 1972, pp. 6–118, 6–160.

[28] A. P. Lenham and D. M. Treherne, "Applicability of the anomolous skin-effect theory to the optical constants of Cu, Ag, and Au in the infrared," *J. Opt. Soc. Amer.*, vol. 56, p. 683, 1960.

[29] S. H. Jensen, "Transient response of non-linear ring resonators using GaAs with photon energy below the band gap," in *SPIE Proc.*, vol. 321, to be published.

George I. Stegeman (M'73) was born in Edinburgh, Scotland, on August 4, 1942. He received the B.A.Sc. degree in 1965 in engineering science, the M.Sc. degree in 1966, and the Ph.D. degree in 1969 in physics, all from the University of Toronto, Toronto, Ont., Canada.

From 1970 to 1980 he was a member of the Faculty of the Department of Physics, University of Toronto. He is currently a Professor at the Optical Sciences Center, University of Arizona, Tucson. He has published over 100 papers in the general area of linear and nonlinear wave interactions at surfaces, both theory and experiment. His current interests include integrated and fiber optics, nonlinear optical and acoustical phenomena, nonlinear signal processing, nonlinear surface polariton interactions, Brillouin scattering at surfaces, surface CARS, and bistability. He is the recipient of the 1980 Hertzberg medal of the Canadian Association of Physicists.

Dr. Stegeman is a member of the American Physical Society, the Canadian Association of Physicists, and a Fellow of the Optical Society of America. He has served as President of the Optics Division of the CAP, the meeting Chairman in 1977, and a Vicechairman of the 1982 annual OSA meetings. He is currently on the Editorial Board of Wave Electronics.

Fiber Optic Measuring System for Electric Current by Using a Magnetooptic Sensor

KAZUO KYUMA, SHUICHI TAI, MASAHIRO NUNOSHITA, TAKASHI TAKIOKA, AND YOSHIAKI IDA

Abstract—A practical fiber optic measuring system for heavy electric current was developed by using the magnetooptic (Faraday) material. In order to obtain better SNR and smaller temperature dependence, the most suitable combination of the light source and Faraday material was experimentally and theoretically determined. Consequently, it was emphasized that an LED and diamagnetic SF-6 flint glass gave the superiority of overall system capability over LD's and para- or ferromagnetics. A novel type of fiber optic current sensor was constructed of the Faraday rotator of SF-6 flint glass with two thin-film polarizers. By using this sensor and a high radiance LED, high accuracy within ±0.5 percent was obtained for magnetic field between 20 and 500 Oe, and at temperatures from -25°C up to 80°C.

I. Introduction

A conventional technique for measuring the electric ac current in high-voltage power systems is based on inductive current transformers (CT's). However, with the recent growing demand for operating on higher voltage in such electric systems, the difficulty of isolation has sharply raised the production cost of CT's. For such demand, fiber optic current sensors are very promising because optical fibers are good isolators and suffer no electromagnetic interference.

There are some requirements for putting such sensors into practical use. With wide dynamic measuring range, the high accuracy within ±1 percent for operating temperatures from -20 to 80°C are required. Other requests for the sensors are small size, high reliability, and low cost.

Fiber optic current sensors are classified into the following three categories: 1) an interferometric sensor utilizing a single-mode fiber coated by magnetostrictive jacket [1], [2], 2) a sensor utilizing the Faraday effect of a single-mode fiber [3], and 3) a sensor constructed of a Faraday material and multimode fibers [4]. The major problem of types 1) and 2) is so sensitive to environmental variations such as temperature or pressure that they cannot satisfy the required accuracy.

In this work, the sensor of type 3) is developed. First, the optimum combination of the Faraday material and the light source is determined to obtain the required performances. Second, a novel integrated structure of current sensors constructed of thin-film polarizers and a Faraday rotator as one body is proposed. The principle and the basic performances of the current measuring system using this sensor are described in detail.

Manuscript received March 4, 1982; revised April 26, 1982.

K. Kyuma, S. Tai, and M. Nunoshita are with the Central Research Laboratory, Mitsubishi Electric Corporation, 80 Nakano, Minamishimisu, Amagasaki, Hyogo, 661 Japan.

T. Takioka and Y. Ida are with the Itami Works, Mitsubishi Electric Corporation, 80 Nakano, Minamishimizu, Amagasaki, Hyoto, 661 Japan.

II. Principle

Fig. 1 shows a schematic configuration of our measuring system. The light of constant intensity is guided from the suitable light source such as a light emitting diode (LED) to the optical current sensor through the incoming optical fiber. The sensor consists of two graded-index rod lenses (5.5 mm long and 1.5 mm in diameter), a polarizer, a Faraday rotator, and an analyzer. The light beam emitted from the incoming fiber is almost collimated by the graded-index rod lens and linearly polarized through the polarizer. The polarized direction of light is rotated in the transparent Faraday material under the influence of the magnetic field. The rotation angle φ is given by

$$\varphi = VHL \tag{1}$$

where V is the Verdet constant, L is the optical path length of the Faraday rotator, and H is the ac magnetic field generated by the electric current in a conductor. Since H is in proportion to the current, φ is also directly proportional to the current. Such polarization modulation due to the Faraday effect is converted into intensity modulation by using the optical analyzer. The maximum sensitivity and linearity of

0018-9480/82/1000-1607$00.75